

Adaptive femtosecond pulse shaping to control supercontinuum generation in a microstructure fiber

D. Lorenc^{a,b,*}, D. Velic^{a,c}, A.N. Markevitch^d, R.J. Levis^d

^a International Laser Centre, Ilkovicova 3, 812 19 Bratislava, Slovakia

^b Department of Nuclear Physics and Biophysics, Faculty of Mathematics, Physics and Computer Science, Comenius University, 842 48 Bratislava, Slovakia

^c Department of Physical and Theoretical Chemistry, Faculty of Natural Sciences, Comenius University, 842 15, Bratislava, Slovakia

^d Department of Chemistry, CAPR, Temple University, Philadelphia, PA 19122, USA

Received 19 July 2006; received in revised form 20 March 2007; accepted 12 April 2007

Abstract

Efficient confinement of laser radiation in the core of a photonic crystal fiber increases the nonlinear processes resulting in supercontinuum generation. The technique of adaptive pulse shaping using an evolutionary algorithm provides a method to gain control over such highly nonlinear processes. Adaptive pulse shaping of the driving laser radiation passing through the photonic crystal fiber is employed to modify the shape and composition of the output supercontinuum. Amplitude and phase shaping are used to optimize the broadband emission between 500 and 700 nm, as well as a soliton centered at 935 nm. The intensities of the emission and of the soliton driven by a shaped laser pulse increase in comparison to an unshaped pulse by factors of 4 and 3, respectively. The spectral width in the range of 500–600 nm is increased by approximately 40%. In addition, the suppression of self-steepening effects in supercontinuum spectra is demonstrated.

© 2007 Elsevier B.V. All rights reserved.

Keywords: Photonic crystal fiber; Pulse shaping; Supercontinuum generation; Soliton

1. Introduction

The field of photonic crystal fibers [1,2] has provided a broad range of technological applications including frequency metrology [3], optical coherence tomography [4], pulse compression [5,6], and nonlinear spectroscopy [7]. One of the most appealing outcomes is the possibility to use sub-nJ femtosecond pulses in order to generate broadband supercontinuum [8]. This phenomenon is facilitated by efficient confinement of light in the small area of the fiber core with high peak intensities of up to 10^{12} W/cm² sustained along an extended interaction length. The process of supercontinuum generation consists of several coupled

nonlinear effects including self-phase modulation [9], Raman scattering, four-wave mixing [10], third harmonic generation [11,12], soliton formation and fission [13]. These nonlinear effects are highly sensitive to the incident pulse amplitude and spectral profile. In this work, the laser pulses were tailored in spectral phase and amplitude space using a pulse shaper to control the desired nonlinear process in the fiber in order to prepare specific supercontinuum spectra.

The pulse shaping technique [14] is an elegant way of controlling the amplitude and phase of an ultrafast laser pulse in the real time. The method has been employed in selective control of chemical processes [15], multiphoton and Raman transitions [16,17], high harmonic generation [18], as well as nonlinear processes in microstructure fibers [19,20]. There are basically two regimes of using the pulse shaper with evolutionary control algorithms [21]. Either “initial knowledge” of the system is available providing an estimate of the pulse temporal envelope and phase

* Corresponding author. Address: International Laser Centre, Ilkovicova 3, 812 19 Bratislava, Slovakia. Tel.: +421 2 654 21 575; fax: +421 2 654 23 244.

E-mail address: lorenc@ilc.sk (D. Lorenc).

functions or an initial set of random masks can be imposed on the pulse shaper. However, in both cases, the evolutionary algorithm searches a sizable parameter space and uses measurements evaluated with a fitness function to optimize the solutions. The adaptive pulse shaping technique has been shown to be a useful and sensitive tool for altering the evolution and subsequent output characteristics of the incident pulse [19]. Instead of using “phase only” pulse shaping [19], both the phase and amplitude were modulated in this work to achieve optimal control over spectral composition of supercontinuum. This additional amplitude shaping allowed us to observe higher optimization factors than those reported before [19] and to improve the control of both solitonic and broadband non-solitonic features in optical spectrum at the output of the microstructure fiber.

2. Experiment

The experimental setup was based on a Ti:Sapphire oscillator seeding a regenerative amplifier that provided a 40 fs pulse train with a repetition frequency of 1 kHz and a central wavelength of 800 nm. The output beam was down-collimated by an all reflective telescope and subsequently entered the reflective mode pulse shaper. The pulse was synthesized using both the amplitude and phase shaping and the resulting beam was focused onto the input facet of a microstructure fiber using a high numerical aperture 60× objective. The sample was a solid core photonic crystal fiber having a core diameter of 4.4 μm and air cladding. The average energy of the femtosecond pulses coupled into the 6 cm long sample was approximately 50 nJ with a coupling efficiency estimated to be 30%. Frequency-resolved optical gating was used to characterize the shaped pulses before entering the fiber.

The supercontinuum spectra produced in the fiber by the shaped pulse were sampled using a modified fiber coupled spectrometer. For the control loop, the analog signal out of the spectrometer was connected to the signal channel of an oscilloscope. An initial set of 40 random masks was prepared with eight pixels tied together to reduce a size of search space [22]. The spectral features of interest were identified and maximized or minimized using the fitness function

$$F = \int_{\lambda_1}^{\lambda_2} I(\lambda) d\lambda \quad (1)$$

where $I(\lambda)$ is the spectral intensity. The fitness function was calculated for each spectrum corresponding to a specific mask and the best masks were chosen using proportional selection for propagation. New masks were generated using operators including mutation and crossover with 2.5% mutation rate.

3. Results and discussion

The dependence of self-steepening on pulse shape [9,19] was initially examined. Self-steepening is a nonlinear process which alters the temporal profile of the pulse. The high

intensity peak is temporally delayed relative to the lower intensity trailing edge. This process results in the steepening of the pulse envelope followed by asymmetric shift of the spectrum caused by the self-phase modulation process. The self-steepening process is assumed to be effective even at a distance of only a fraction of the nonlinear length [9]

$$L_{NL} = 1/\gamma P_0 \quad (2)$$

where γ is the nonlinear parameter of the fiber sample and P_0 is the peak power of incident pulse. The characteristic self-steepening parameter is defined as

$$s = T_{opt}/2\pi T_0 \quad (3)$$

where T_{opt} is the optical period and T_0 is the pulse duration. In our case the characteristic ratio becomes

$$sL/L_{NL} \sim 3 \quad (4)$$

where L denotes the sample length. In order to estimate the relevance of self-steepening process a shock distance is defined for Gaussian pulses as

$$z_s = 0.39L_{NL}/s \quad (5)$$

Eq. (5) is valid for the dispersionless case and loss-free fiber. In order to gain a deeper understanding of fiber dispersion characteristics, finite difference beam propagation [23] simulation was performed. The spectral dependence of dispersion parameter was calculated for the three lowest order modes i.e., fundamental, first-order and second-order mode as shown in Fig. 1a–c, respectively. Modes higher than the fundamental mode only had to be considered to explain the solitonic phenomena observed. Moreover, efficient coupling into the higher-order modes apparently occurred during supercontinuum generation. Based on the simulation shown in Fig. 1, our fiber sample had the zero dispersion wavelength close to 910 nm for the fundamental mode. Under these conditions, self-steepening was dominated by losses in the fiber [9]. Our sample with L_{NL} of approximately 0.2 mm, z_s of 8 mm and the sample length

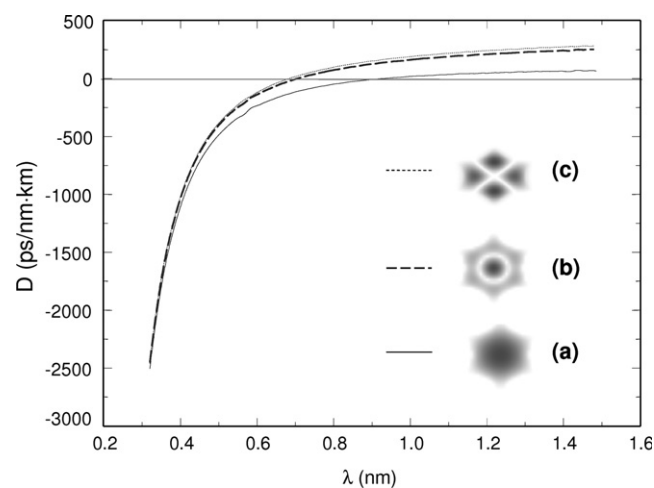


Fig. 1. Calculated variation of dispersion parameter as a function of wavelength for the three lowest order fiber modes (a, b, c).

of 60 mm allowed efficient self-steepening to be observed. The self-steepening process therefore caused the output supercontinuum to become strongly asymmetric and undulating. A degree of precompensation was needed to correct this behavior. Obviously, the correction can be accomplished by placing the steepness on the leading edge of the incident pulse. In order to verify this approach, the spectra were compared in the cases of pulses being forward and backward ramped [19]. In the case of forward ramped pulse, the steepening was placed at the leading temporal edge of the laser pulse, whereas, in the case of backward ramped pulse, the steepening was placed at the trailing temporal edge. The temporal pulse shapes for forward and backward ramped pulses are shown in Fig. 2 along with the FROG traces shown in the inset. The supercontinuum spectra obtained by using forward and backward ramped pulses are shown in Fig. 3. The forward ramped pulse generated the most symmetric spectrum with suppressed oscillations. The backward ramped pulse generated a larger blue shift and considerable deep oscillations in the output spectra. The asymmetry in the output spectrum resulted from the asymmetry in the temporal shape of the self-steepened pulse. Consequently, enhanced spectral broadening was observed at the steep trailing edge of the pulse where blue spectral components were generated through the self-phase modulation. The observation is consistent with the previously obtained [19] theoretical and experimental data.

The adaptive algorithm was used to optimize specific features in the supercontinuum range between 500 and 700 nm. Optimization of broadband features in the supercontinuum is of interest to achieve a smoother, broader, and more intense spectra in distinct regions. The original and optimized spectra are compared in Fig. 4. This optimization experiment resulted in an increase of spectral intensity in the range of 600–700 nm by a factor of four. The effective width of the broadband feature in the range of 500–600 nm was also increased by approximately 40%.

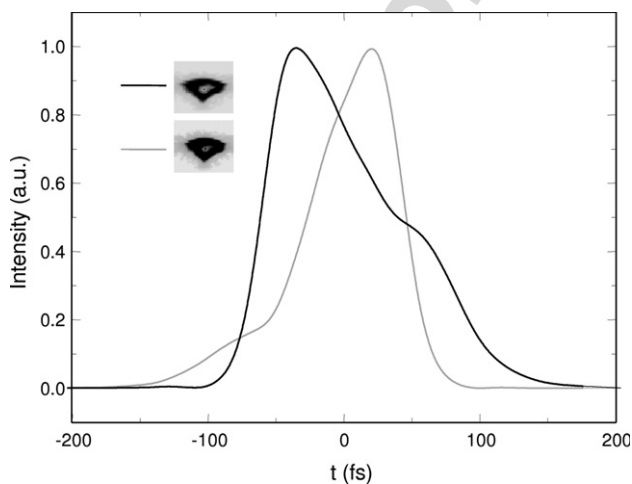


Fig. 2. Temporal pulse shapes and FROG traces of forward ramped (black) and backward ramped (gray) pulses.

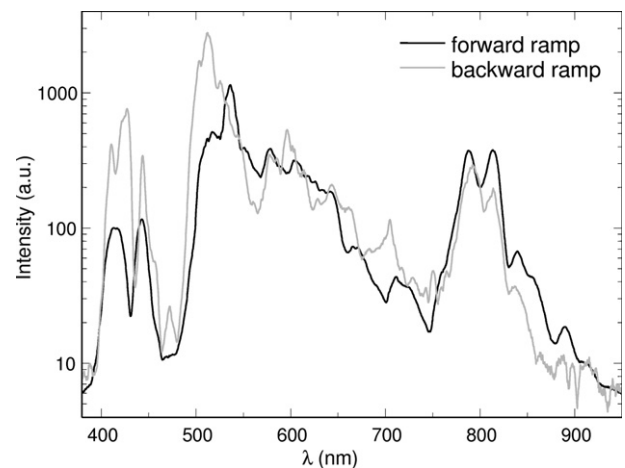


Fig. 3. Supercontinuum spectra obtained with forward ramped (black) and backward ramped (gray) pulses.

Not only the increases of the width and intensity were observed, but also the two originally isolated features at approximately 700 nm were merged into a smoother spectrum. The broadband features in the 500–700 nm spectral region are most probably a result of four-wave mixing process. Effective coupling to the higher order modes was observed in this experiment. As shown in Fig. 1, central wavelength of the pump is in the anomalous dispersion regime for higher-order modes, creating favorable conditions for the self-phase modulation phase matched four-wave mixing [9]. Both the temporal shapes and phases were acquired for the pulse before and after the optimization. As shown in Fig. 5, the predominant effect of the adaptive pulse shaping procedure was to change the sign of the temporal phase in such a way as to put it in a favor of self-phase modulation. The optimal phase effectively mimics the phase profile produced by self-phase modulation, thus enhancing its nonlinear influence. After the optimization, the enhanced nonlinear self-phase modulation term effectively compensates for all the other mismatch terms. As a

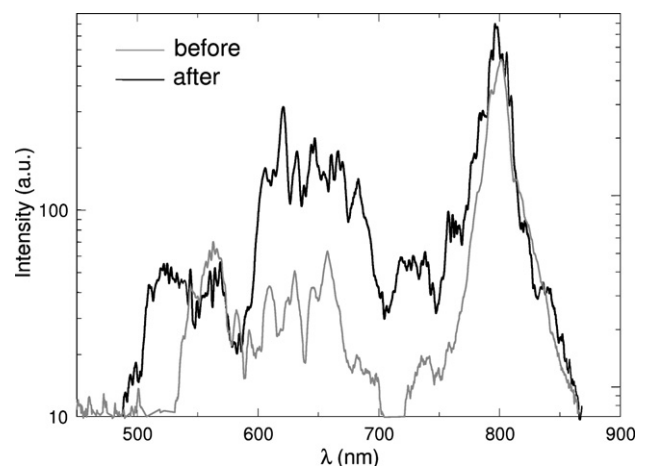


Fig. 4. Supercontinuum spectra before (gray) and after (black) the optimization of the spectral features in the range from 500 to 700 nm.

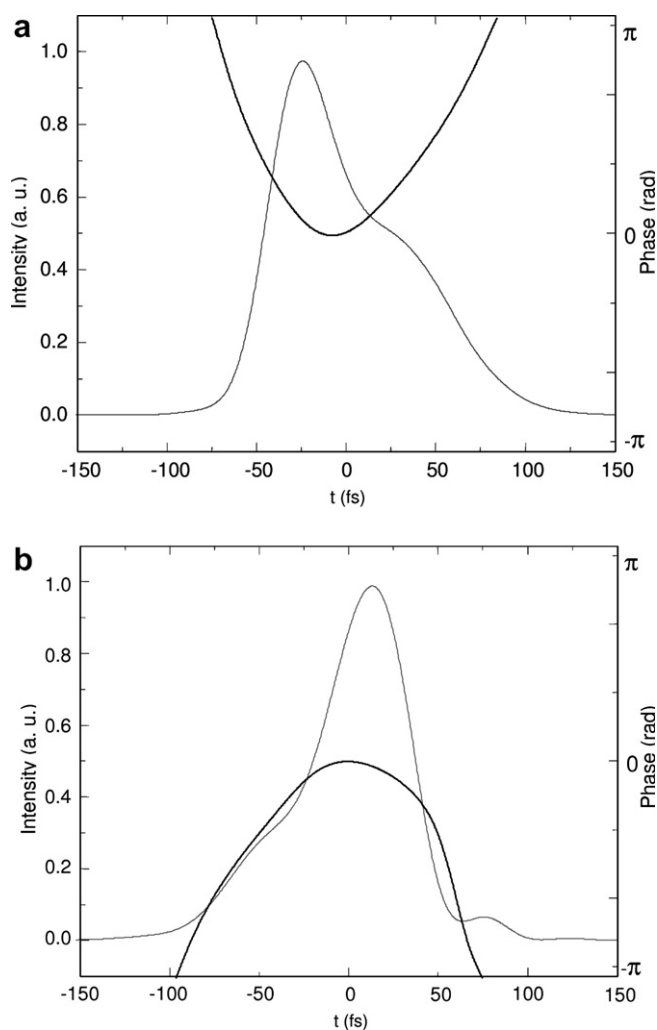


Fig. 5. Temporal pulse shapes (gray) and phases (black) for the optimization of 500–700 nm spectral region: the initial pulse (a) and the optimized pulse (b).

result, frequency shifted spectral sidebands [9] Ω_s are generated. Indeed, approximate calculations of the frequency shift Ω_s provided values of $1\text{--}3 \times 10^{14}$ Hz being in reasonable agreement with the 500–700 nm spectral region.

The optimization curve shown in Fig. 6 was obtained and its fluctuation is most probably due to fluctuations in laser power and phase as a result of thermal drifts. The corresponding power fluctuation of the laser system is shown in the lower part of Fig. 6. Comparing the two curves, there is no clear correspondence between fluctuations in optimization curve and laser system output power. There are several sources of fluctuation, one of them could be the variation of temperature coincident to the air-conditioning loop operation. Since the processes leading to supercontinuum generation are of highly nonlinear nature, there was a strong coupling between the supercontinuum spectra and variations, both in the phase and amplitude of the incident pulse. Moreover, since the duration of a typical optimization run was rather long, both the long term and short term stabilities of the laser source were crucial. Nevertheless, a clear improvement of the optimized value with the increase

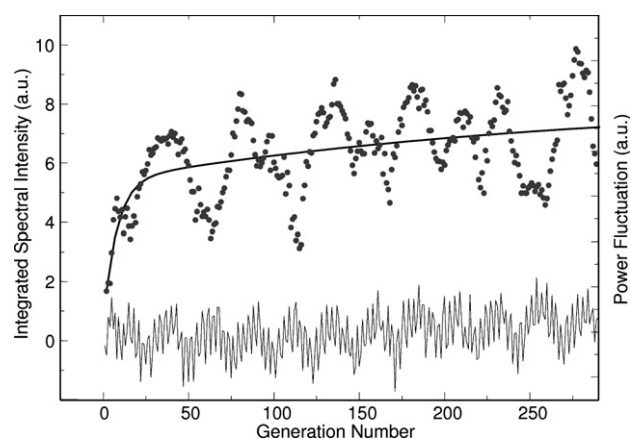


Fig. 6. Optimization of supercontinuum spectrum in the 500–700 nm range (data points). The thick curve is the exponential fit to experimental data. Below, fluctuations of laser power during the optimization run are shown (black line).

in the spectral intensity by a factor of four was observed after approximately 50 generations.

The selective control of the amplitude of a soliton at approximately 935 nm was investigated. Soliton self-frequency shift [24] was also observed due to Raman self-pumping of the soliton which continuously transfers energy from shorter to longer wavelengths. The transfer causes a red shift of the pulse center wavelength. To explain solitonic behavior, higher order modes have to be considered. Indeed, higher order modes were observed at the output of the sample during supercontinuum generation. Note that the 800 nm central wavelength of incident pulse was near the zero dispersion wavelength for the first- and second-order modes in the anomalous dispersion region of the sample as shown in Fig. 1. Therefore, the soliton formation, soliton self-frequency shift and soliton fission are assumed to play important roles in supercontinuum generation [14]. Both the initial and optimized spectra are shown in Fig. 7. The soliton at 935 nm was optimized and the

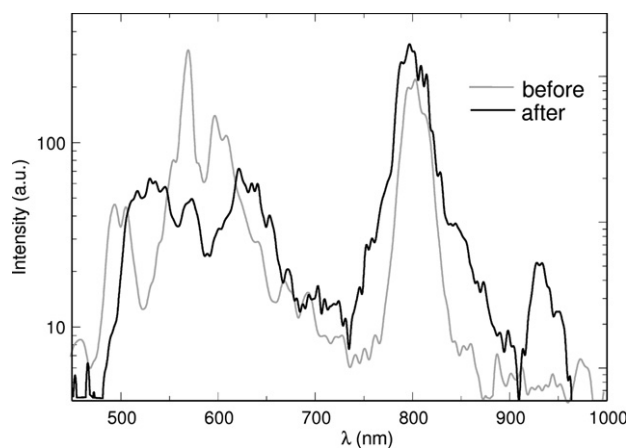


Fig. 7. Supercontinuum spectra before (gray) and after (black) the optimization with the focus on the soliton centered at 935 nm.

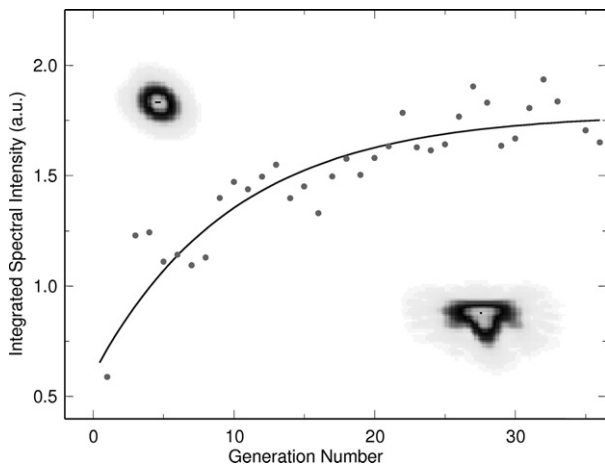


Fig. 8. Optimization datapoints (gray) for the soliton along with the exponential fit (black). FROG traces of the unshaped pulse and optimized pulse are shown in the upper left and lower right corners, respectively.

corresponding optimization curve is shown in Fig. 8. The improvement of integrated intensity was measured to be a factor of three. FROG traces of the initial and optimized driving pulses for soliton formation are shown in the inset of Fig. 8. Considering the importance of solitons for present and future photonics applications, the ability to control their properties is important.

4. Conclusions

The pulse shaping method was demonstrated to be a useful tool to achieve specific tasks in supercontinuum generation inside of the microstructure fiber. Ramping of incident pulse allowed compensation for the asymmetry in the supercontinuum spectrum caused by self-steepening process. Optimization of broad spectral region in the supercontinuum ranging from 500 to 700 nm was performed with a 40% increase of the spectral width in the range of 500–600 nm and improvement of spectral intensity by a factor of four in the range of 600–700 nm. The two originally separated spectral regions at approximately 700 nm eventually merged into the smoother, broader, and more intense supercontinuum. The spectral intensity of the soliton at 935 nm was improved by a factor of three. The use of evolutionary algorithm and adaptive pulse shaping provides the possibility to either enhance or to suppress specific features in the spectrum of supercontinuum and thereby to enhance the control over spectral composition in a straightforward way.

Acknowledgements

The authors acknowledge the financial support of APVT-20-029804, VEGA 1/3577/06, the Department of Defense MURI Program, as managed by the Army Research Office, and the Air Force Office for Scientific Research DARPA Program. The authors are grateful to A.M. Zheltikov for the fiber sample.

References

- [1] J.C. Knight, T.A. Birks, P.St.J. Russell, D.M. Atkin, *Opt. Lett.* 21 (1996) 1547.
- [2] T.A. Birks, J.C. Knight, P.S. Russell, *Opt. Lett.* 22 (1997) 961.
- [3] D.J. Jones, S.A. Diddams, J.K. Ranka, A. Stentz, R.S. Windeler, J.L. Hall, S.T. Cundiff, *Science* 288 (2000) 635.
- [4] I. Hartl, X.D. Li, C. Chudoba, R.K. Ghanta, T.H. Ko, J.G. Fujimoto, J.K. Ranka, R.S. Windeler, *Opt. Lett.* 26 (2001) 608.
- [5] T. Suedmeyer, F. Brunner, E. Innerhofer, R. Paschotta, K. Furusawa, J.C. Baggett, T.M. Monro, D.J. Richardson, U. Keller, *Opt. Lett.* 28 (2003) 1951.
- [6] E. Seres, R. Herzog, J. Seres, D. Kaplan, C. Spielmann, *Opt. Express* 11 (2003) 240.
- [7] A.B. Fedotov, P. Zhou, A.P. Tarasevitch, K.V. Dukelskij, Y.N. Kondratev, V.S. Shevandin, V.B. Smirnov, D. von der Linde, A.M. Zheltikov, *J. Raman Spectrosc.* 33 (2002) 888.
- [8] J.K. Ranka, R.S. Windeler, A.J. Stentz, *Opt. Lett.* 25 (2000) 25.
- [9] G.P. Agrawal, *Nonlinear Fiber Optics*, Academic Press, San Diego, 2001.
- [10] S. Coen, A.H.L. Chau, R. Leonhardt, J.D. Harvey, J.C. Knight, W.J. Wadsworth, P.St.J. Russell, *J. Opt. Soc. Am. B* 19 (2002) 753.
- [11] F.G. Omenetto, A.J. Taylor, M.D. Moores, J. Arriaga, J.C. Knight, W.J. Wadsworth, P.St.J. Russell, *Opt. Lett.* 26 (2001) 1158.
- [12] L. Tartara, I. Christiani, V. Degiorgo, F. Carbone, D. Faccio, M. Romagnoli, W. Belardi, *Opt. Commun.* 215 (2003) 191.
- [13] J. Herrmann, U. Griebner, N. Zhavoronkov, A. Husakov, D. Nickel, J.C. Knight, W.J. Wadsworth, P.St.J. Russell, G. Korn, *Phys. Rev. Lett.* 88 (2002) 173901.
- [14] A.M. Weiner, *Rev. Sci. Instr.* 71 (2000) 1929.
- [15] R.J. Levis, G.M. Menkir, H. Rabitz, *Science* 292 (2001) 709.
- [16] D. Meshulach, Y. Silberberg, *Nature* 396 (1998) 239.
- [17] D. Oron, N. Dudovich, D. Yelin, Y. Silberberg, *Phys. Rev. A* 65 (2002) 043408.
- [18] R. Bartels, S. Backus, E. Zeek, L. Misoguti, G. Vdovin, I.P. Christov, M.M. Murnane, H.C. Kapteyn, *Nature* 406 (2000) 164.
- [19] S. Xu, D.H. Reitze, R.S. Windeler, *Opt. Express* 12 (2004) 4731.
- [20] B. Von Vacano, W. Wohlleben, M. Motzkus, *Opt. Lett.* 31 (2006) 413.
- [21] D. Zeidler, S. Frey, K.L. Kompa, M. Motzkus, *Phys. Rev. A* 64 (2001) 023420.
- [22] R. Mizoguchi, K. Onda, S.S. Kano, A. Wada, *Rev. Sci. Instr.* 74 (2003) 2670.
- [23] R. Scarmozzino, A. Gopinath, R. Pregla, S. Helfert, *J. Selected Topics in Quantum Electronics* 6 (2000) 150.
- [24] D.T. Reid, I.G. Cormack, W.J. Wadsworth, J.C. Knight, P.St.J. Russell, *J. Mod. Optics* 49 (2002) 757.